

Yttrium Tantalum Oxynitride Multiphases as Photoanodes for Water Oxidation

Wenping Si,^{†,‡} Zahra Pourmand Tehrani,[†] Fatima Haydous,[†] Nicola Marzari,[§] Ivano E. Castelli,^{//}
Daniele Pergolesi,^{*,†,⊥} and Thomas Lippert^{*,†,#}

[†]Laboratory for Multiscale Materials Experiments, Paul Scherrer Institut, 5232 Villigen PSI, Switzerland. [‡]Key Laboratory of Advanced Ceramics and Machining Technology, Ministry of Education, School of Materials Science and Engineering, Tianjin University, Tianjin 300072, P.R. China. [§]Theory and Simulation of Materials (THEOS) and National Centre for Computational Design and Discovery of Novel Materials (MARVEL), École Polytechnique Fédérale de Lausanne, 1015 Lausanne, Switzerland. ^{//}Department of Energy Conversion and Storage, Technical University of Denmark, Fysikvej 309, DK-2800 Kgs. Lyngby, Denmark. [⊥]Electrochemistry Laboratory, Paul Scherrer Institut, 5232 Villigen-PSI, Switzerland. [#]Laboratory of Inorganic Chemistry, Department of Chemistry and Applied Biosciences, ETH Zurich, 8093 Zurich, Switzerland.

●, *Supporting Information*

ABSTRACT: Perovskite yttrium tantalum oxynitride is theoretically proposed as a promising semiconductor for solar water splitting because of the predicted bandgap and energy positions of band edges. In experiment, however, we show here that depending on processing parameters, yttrium tantalum oxynitrides exist in multiphases, including the desired perovskite YTaN_2 , defect fluorite $\text{YTa}(\text{O},\text{N},\square)_4$, and N-doped YTaN_4 . These multiphases have bandgaps ranging between

2.13 and 2.31 eV, all responsive to visible light. The N-doped YTaO₄, perovskite main phase, and fluorite main phase derived from crystalline fergusonite oxide precursors exhibit interesting photoelectrochemical performances for water oxidation, while the defect fluorite derived from low crystallized scheelite-type oxide precursors show negligible activity. Preliminary measurements show that loading IrO_x cocatalyst on N-doped YTaO₄ significantly improves its photoelectrochemical performance encouraging further studies to optimize this new material for solar fuel production.

■ INTRODUCTION

Photoelectrochemical (PEC) water splitting driven by solar light offers promises as a clean and effective method to convert solar energy into chemical energy in the form of hydrogen as renewable fuel. The PEC water splitting process includes the absorption of a photon by a semiconductor to create an electron-hole pair, the separation and migration of the two particles to the surface of the semiconductor to oxidize/reduce water into O₂ and H₂.

To utilize as much as possible solar light, many efforts have been dedicated to develop semiconductor photocatalysts with light absorption extended to the visible spectrum region. Under this perspective, many oxynitrides are promising photocatalyst materials. Compared to the pristine oxides, the bandgaps of many oxynitrides are within the visible light region due to an upward shift in the valence band edge as a consequence of the hybridization of the O 2p and N 2p orbitals.¹⁻⁸ In some case, the N substitution also shifts the conduction band edge downward, therefore contributing to the overall reduction of the band gap.⁷

Recent theoretical studies report the result of a computational screening of thousands of possible compositions of perovskite oxynitrides based on the structural stability, the bandgap width, and

positions of band edges, which indicates YTaON₂ as a promising semiconductor for solar water splitting.⁹⁻¹⁰ The structural stability of this compound is however still a controversial issue since other studies predict the perovskite YTaON₂ to be structurally unstable as far as the tolerance and octahedral factors are concerned.¹¹ In literature, only traces of the perovskite structure were experimentally obtained after ammonolysis of the precursor YTaO₄, whereas in most cases, defect fluorite YTa(O,N,□)₄ (where □ denotes a vacancy) were the main products.¹²⁻¹⁶ Although Muraoka et al.¹⁶ labelled the ammonolysis product as pyrochlore Y₂Ta₂O₅N₂, the XRD pattern clearly indicates the fluorite type structure with no sur-structure peaks as expected in the case of the pyrochlore phase for larger rare-earth elements.

Inspired by theoretical predictions and based on the available experimental results, we report here a thorough study of the ammonolysis of YTaO₄ (Y: Ta = 1 ratio) to revisit and clarify the preparation and PEC performances of the Y-Ta-O-N system for water oxidation.

The literature shows that structure and morphology of the precursor oxide can significantly affect the ammonolysis process.¹⁷ For this reason, in this work, both low crystallized scheelite-type oxide and crystalline fergusonite YTaO₄ are used as oxide precursors, prepared by the polymerized complex method and solid state reaction, respectively. Ammonolysis under various temperatures and ammonia flows are used in experiment, resulting in a series of oxynitrides with different crystalline structures and bandgaps. PEC measurements are conducted to examine the photoactivity towards water oxidation of the obtained compounds.

■ EXPERIMENTAL SECTION

Preparation of yttrium tantalum oxynitride

Preparation of the oxide precursor YTaO₄: Two methods have been utilized to prepare the oxide precursor in this system. 1) Polymerized complex method (PC): To prepare the oxide precursors, Y(NO₃)₃·6H₂O (Alfa Aesar, 99% Reactor) and TaCl₅ (Chempur, 99.99%) were dissolved in methanol (VWR Chemicals) with the addition of citric acid (Sigma, ≥99%) and ethylene glycol (Aldrich, 99.8%) (citric acid and ethylene glycol were added in the solution as concentration ratio of [Y]: [Ta]:[Citric acid]: [ethylene glycol]=1:1:5:20). The solution was stirred at 200 °C to promote polymerization, and eventually a transparent gel was formed with uniformly dispersed constituent elements. Afterwards, the gel was transferred to an alumina crucible and heated at 750 °C for 5 h in air, resulting in low crystallized scheelite-type YTaO₄ powders. 2) Solid state reaction method (SSR): Y₂O₃ (Alfa Aesar, 99.99%, Reactor) powders and Ta₂O₅ (Alfa Aesar, 99.993%, Puratronic) powders were used as the precursors to prepare crystalline fergusonite YTaO₄. Y₂O₃ and Ta₂O₅ powders in a stoichiometric ratio of 1:1 were mixed and grinded for 1h, and then pressed into a pellet, which was heated at 900 °C for 2 h and then at 1400 °C for 10 h. In order to get single phase YTaO₄, this procedure was repeated four times.

Preparation of yttrium tantalum oxynitride through thermal ammonolysis: 0.15 g of the oxide precursor were put in an alumina boat and placed in a tube furnace through which ammonia gas flowed at a rate of 50 mL min⁻¹ or 220 mL min⁻¹. Various temperatures between 850 °C and 950 °C have been used to prepare different structures. NaCl, KCl and NH₄Cl were also tried as a mineralizer for the ammonolysis.

Materials characterizations

X-ray diffraction (XRD) characterizations of the yttrium tantalum oxides and oxynitrides were conducted using a Bruker–Siemens D500 X-ray powder diffractometer equipped with Cu K α

radiation (1.5418 Å) and a scintillation counter detector. θ - 2θ scans were performed with a step increment of 0.01 ° at a speed of 1 s per step. A Cary 500 Scan UV–Vis–NIR spectrophotometer equipped with an integrating sphere was used to measure the diffuse reflectance of the powders to obtain the band gaps. The measured reflectance was converted to Kubelka–Munk function, and the band gap magnitudes were estimated by extrapolating the absorption edge to the ground level. Scanning electron microscopy (SEM) images were obtained with a Zeiss Supra VP55 Scanning Electron Microscope. The N content of the oxynitride powders was determined by thermogravimetric (TG) analysis from the mass difference between the oxynitride and the resulting oxide after heating in synthetic air. The TG measurements were acquired using a NETZSCH STA 449C analyzer equipped with PFEIFFER VACUUM ThermoStar mass spectrometer, where oxynitride powders were heated in alumina crucibles to 1400 °C with a heating rate of 10 °C min⁻¹ in 36.8 mL min⁻¹ synthetic air.

Photoanode preparation

Yttrium tantalum oxynitride photoanodes were prepared *via* the electrophoretic deposition method (EPD) followed by a necking treatment.¹⁸ In detail, 120 mg yttrium tantalum oxynitride powders were dispersed in 50 mL acetone with 10 mg iodine and sonicated for 60 min. The yttrium tantalum oxynitride powders were positively charged due to the releasing of H⁺ when iodine reacted with acetone. Two parallel FTO substrates ($\sim 7 \Omega \text{ sq}^{-1}$, Sigma Aldrich) were then placed in the oxynitride dispersion with a distance of 1 cm under a bias of 20 V for 5 min. Yttrium tantalum oxynitride powders were deposited on the negative electrode. The so-called necking treatment was then applied to the electrode to improve the electronic conduction between oxynitride particles and the FTO substrate. Yttrium tantalum oxynitride photoanodes were treated with 25 μL of 10 mM TaCl₅ methanol solution and dried in air. This procedure was repeated for three times, followed

by heating at 350 °C in air for 30 min. This temperature was chosen to avoid oxidation of the oxynitrides.

Cocatalyst IrO_x was post-loaded on the oxynitride photoanodes by impregnation from a colloidal IrO₂ aqueous solution, which was prepared by hydrolysis of Na₂IrCl₆.¹⁹ The colloidal IrO₂ was prepared as follows: 50 mL H₂O was used to dissolve 0.008 g Na₂IrCl₆·6H₂O, the pH of which was adjusted to 11–12 with 1 M NaOH. The solution was heated at 80 °C for 30 min and cooled to room temperature by immersion in an ice water bath. HNO₃ was used to adjust the pH of the cooled solution to 10. A blue solution containing colloidal IrO₂ was obtained by subsequent heating at 80 °C for 30 min. The photoanodes were immersed in the IrO₂ colloid for 30 min, heated at 300 °C for 30 min and then washed with distilled water before PEC measurements.

PEC measurements

PEC measurements were performed in a three electrode configuration in 0.5 M NaOH (pH=13.0) aqueous solution. The yttrium tantalum oxynitride photoelectrode was used as the working electrode; a coiled Pt wire and Ag/AgCl were used as the counter and reference electrodes, respectively. To simplify the display of the working electrode potential, V_{RHE} (potential vs. reversible hydrogen electrode) was adopted throughout the manuscript, which was obtained according to the Nernstian relation. A Solartron 1286 electrochemical interface was used to carry out the voltage scan and current collection. Potentiodynamic measurements with a scan rate of 10 mV s⁻¹ in the potential window of 0.5–1.7 V_{RHE} were performed to investigate the PEC performance of Y-Ta-O-N multiphases. The chopped dark–light current densities were normalized according to the illuminated area. The light source was a 150 W Xe lamp equipped with an AM 1.5G filter (100 mW cm⁻², Newport 66477-150XF-R1) calibrated by a photodetector (Gentec-EO).

■ RESULTS AND DISCUSSION

Structural analysis of Y-Ta-O-N multiphases

As shown in Figure 1 and consistent with literature,¹² oxide precursors obtained by polymerized complex method were indexed to the XRD pattern of low crystallized scheelite-type YTaO_4 (denoted as LO, PDF #00-050-0846). Various temperatures and the flow rates of ammonia were tested to prepare the oxynitrides. At a high temperature of 950 °C and under a high ammonia flow of 220 mL min⁻¹, yellowish and reddish orange products were obtained after 10 h and 20 h ammonolysis, respectively. The XRD pattern shown in Figure 1 indicates a defect fluorite structure $\text{YTa}(\text{O},\text{N},\square)_4$, as reported in literature.¹² In the following, we refer to these samples as “fluorite-nitride” FN1 and FN2.

In agreement with the available literature,¹² we can confirm that low crystallized scheelite-type YTaO_4 tends to be nitrated into defect fluorite $\text{YTa}(\text{O},\text{N},\square)_4$ at temperatures higher than 900 °C. However, no perovskite structure can be obtained using the low crystallized scheelite-type YTaO_4 precursor.

Solid state reaction method was also used to prepare crystalline fergusonite YTaO_4 (denoted as crystalline oxide CO) as precursor for thermal ammonolysis. The XRD pattern in Figure 2 shows that the obtained YTaO_4 is in fergusonite crystalline structure (PDF #01-072-2018). After 15 h ammonolysis at 850 °C, a yellow product was obtained. The XRD pattern indicates that the crystalline structure of the product remains similar to that of the crystalline oxide precursor, with all diffraction peaks only slightly broadened and shifted towards smaller 2θ angles due to N doping in the lattice. We label this product as N-doped YTaO_4 “NO”.

In addition, a new peak appears at 2θ of $\sim 31.9^\circ$, indicated by the blue arrow in Figure 2, which is similar to the characteristic peak at $\sim 31.3^\circ$ of the perovskite LaTaON_2 (PDF #00-053-0960). And the larger 2θ value of this peak for YTaON_2 is also consistent with the fact that Y has a smaller atomic radius compared to La. This suggests that the nitridation onset temperature is around 850°C . But at this temperature, the reaction is so slow that it takes 100 h of ammonolysis to completely convert the oxides to oxynitrides. The same products can be achieved by ammonolysis at 880°C for 45 h, as shown in Figure 2. In both cases, the products exhibit a yellowish orange color. The XRD patterns confirm that the ammonolysis under 850°C and 880°C result in similar products which are a mixture of perovskite YTaON_2 (main phase), defect fluorite $\text{YTa}(\text{O},\text{N},\square)_4$ and a small trace of Ta_3N_5 . These two products are denoted as PM1 and PM2, where PM stands for “perovskite main phase”.

Increasing the ammonolysis temperature to 950°C also leads to a mixture of perovskite and fluorite oxynitrides, but the XRD pattern suggests that the fluorite is the main phase. We refer to this product as “fluorite main phase” FM. Traces of Ta_3N_5 are also detected by XRD.

Summarizing the results shown in Figure 1 and 2, we conclude that low crystallized scheelite-type YTaO_4 tends to be nitrided into defect fluorite oxynitride. Crystalline fergusonite YTaO_4 tends to form a mixture of perovskite and defect fluorite where the perovskite is the main phase at temperatures lower than 900°C and the fluorite is the main phase at higher temperatures. This is most probably due to the phase transition between fergusonite and scheelite YTaO_4 upon heating.²⁰⁻²³ In fact, three crystal structures exist for YTaO_4 : scheelite (tetragonal, T), fergusonite (monoclinic, M), and a third monoclinic fergusonite form M' , which is very similar to M except for a halved b axis.²⁰⁻²³ T can be obtained at temperature higher than 1450°C , which transforms to M by cooling, while M' structure is obtained when crystals are grown below the M-T

transformation temperature.²⁰ Upon heating, the M' phase transforms sluggishly into T.²⁰⁻²³ In this work, 1400 °C was used to prepare YTaO₄, which actually leads to M'. Thus, upon heating, the M' phase transforms sluggishly into T. At lower ammonolysis temperatures, the transformation from fergusonite YTaO₄ into the scheelite structure is very sluggish and fergusonite is the main phase, resulting in more perovskite main phase in the ammonolysis products. Instead, at an ammonolysis temperature of 950 °C, the transformation of fergusonite YTaO₄ into the scheelite structure becomes faster, leading to more defect fluorite phase in the final oxynitrides.

Chloride salts were examined as mineralizers (also known as flux)²⁴⁻²⁶ in the thermal ammonolysis process. It was found that NaCl and KCl promote the decomposition of binary metal oxides eventually resulting in large amounts of Ta₃N₅.²⁴ Figure S1 in the supporting information shows the results obtained with NaCl. NH₄Cl was also tested as mineralizer but no significant effect was observed. Table 1 shows the summary of the preparation for yttrium tantalum oxides and oxynitrides.

In addition, TG measurements were performed to determine the N contents of the oxynitrides and the results are shown in Figure S2. According to these measurements, the composition of single phase defect fluorite FN2 can be calculated to be YTaO_{2.47}N_{1.01}□_{0.52}, which is very close to the compositions of YTaO_{2.76}N_{0.83}□_{0.41} and YTaO_{2.39}N_{1.08}□_{0.53} for defect fluorite phase reported by Maillard et al.¹² Regarding the samples with main phase NO, FM, and PM1, only the nominal compositions can be considered since these samples are not composed by single phases. The nominal compositions of NO, FM and PM1 are YTaO_{3.32}N_{0.45}, YTaO_{2.18}N_{1.21} and YTaO_{3.01}N_{0.66}, respectively.

Morphologies of Y-Ta-O-N multiphases

SEM images in Figure 3a and b show that FN1, FN2 (i.e. obtained from low crystallized scheelite-type LO) have similar morphologies, consisting of nanoparticles with average sizes of a few tens nm. These nanoparticles agglomerate to form large loosely connected aggregates.

The SEM micrographs of NO, PM1 and FM produced from crystalline precursor CO are shown in Figure 3c, d, and e. They exhibit similar morphologies, but in this case micro-powders with grain sizes in the range of 0.5-3 μm are obtained. It is also noteworthy that the grains of micro-powders show large amounts of cracks and pores, probably formed during the high temperature ammonolysis.

These measurements confirm that the oxide precursors have crucial influence on the final oxynitrides. Similar observations have been reported on other oxynitrides such as LaTiO_2N ,²⁷ LaTaON_2 ,²⁸⁻²⁹ and CaNbO_2N .⁴

UV-Vis absorbance and bandgap

It can be observed visually that the prepared oxynitrides exhibit distinct colors, as listed in Table 1, indicating different bandgaps (E_g). E_g is a very important parameter for light absorption and further photoelectrochemical performances. Diffuse-reflectance absorption spectroscopy was used to estimate E_g for the the fluorite FN1 and FN2, the N-doped YTao_4 NO, the perovskite main phase PM1 and the fluorite main phase FM.

Figure 4 shows the Kubelka-Munk absorbance derived from UV-Vis diffuse reflectance spectrum. FN1 and FN2 obtained from LO exhibit higher absorbance than NO and PM1 obtained from CO. The bandgaps for FN1, FN2, NO, PM1, and FM are 2.25, 2.13, 2.31, 2.23, and 2.26 eV. Considering the correlation of the bandgaps with the samples' thermal history, it is found that the

bandgap tends to decrease with higher ammonolysis temperature and longer reaction time. This is most probably due to a higher N content. Based on the bandgaps, a preliminary DFT calculation was also carried out to search for possible structures and the results are shown in Figure S3.

PEC performance of yttrium tantalum oxynitrides for water oxidation

PEC measurements for water splitting under chopped AM 1.5 G illumination were performed on photoelectrodes prepared by depositing the oxynitride powders on FTO substrates, and the photocurrent densities are shown in Figure 5a. The oxynitrides obtained from low crystallized scheelite-type oxide precursors, i.e. FN1, and FN2, show negligible photoactivity. While NO, PM1, and FM show clearly measurable photoactivity, with photocurrent densities for water oxidation of about $1.0 \mu\text{A cm}^{-2}$, $1.9 \mu\text{A cm}^{-2}$, and $0.6 \mu\text{A cm}^{-2}$ at $1.3 V_{\text{RHE}}$, respectively. Such a different behavior could be ascribed to the different morphologies observed for the two sets of powders, as shown in Figure 3. The much more extended grain boundary region in the nano-powders obtained from low crystallized scheelite-type oxide precursors increases the recombination of photogenerated charge carriers. Muraoka et al.¹⁶ reported evident photocurrents for yttrium tantalum oxynitride obtained from precursors prepared using the PC route. However, the light source for the photoelectrochemical measurement in this reference was different from what is used in the current work. The power density of the irradiated light in the reference was not calibrated, only mentioning the use of a xenon lamp (300 W) with cut-off filters for visible light irradiation ($\lambda > 500 \text{ nm}$). Depending on the distance of the light source and electrodes, a 300 W xenon lamp could give very different power densities, which is directly related with the measured photocurrent density.

To further improve the photocurrent, cocatalysts are used to suppress the surface recombinations of charge carriers and to promote the water oxidation reaction.³⁰ In this study, IrO_x cocatalysts are loaded onto the photoelectrodes and the photocurrents are shown in Figure 5b. The product NO shows a photocurrent density of ~17 μA cm⁻² at 1.3 V_{RHE}, while with PM1 and FM photocurrent densities of ~3.2 μA cm⁻² and ~2.5 μA cm⁻² at 1.3 V_{RHE} were measured. These results indicate that, compared to the mixed phases of PM and FM, NO has better bulk properties in terms of charge separation and conductivity.

The photocurrent density of IrO_x loaded-NO is comparable to those reported in literature for other well-known oxynitrides such as BaTaO₂N,³¹ LaTaON₂,^{6, 29} CaNbO₂N⁴ and Na_xLa_{1-x}TaO_{1+2x}N_{2-2x}.³² The PEC performance of this material could be further improved by optimization of the N content to reduce the bandgap and to enhance the conductivity and by loading more suitable cocatalysts to minimize the loss of surface charge carriers.³¹ N-doped YTaO₄ is indeed a new material that certainly deserves further research studies to fully investigate its potentials for solar water splitting.

■ CONCLUSIONS

In this study, different phases of yttrium tantalum oxynitride are synthesized using low crystallized scheelite-type YTaO₄ and crystalline fergusonite YTaO₄ as the starting oxide precursors. It is found that low crystallized scheelite-type YTaO₄ precursor tends to be nitrated into defect fluorite YTa(O,N,□)₄ nanoparticles. Crystalline fergusonite YTaO₄ precursor tends to be nitrated into micro-powders with mixed crystalline structures including perovskite YTaON₂, defect fluorite YTa(O,N,□)₄ and a small trace of Ta₃N₅. Perovskite exists as the main phase in the product of ammonolysis below 900 °C, while defect fluorite is the main phase above that temperature. In

addition, other multiphases can also be obtained such as N-doped YTaO₄, which can be synthesized starting from the crystalline oxide precursor through a short ammonolysis of 15 h at relatively low temperature of 850 °C. UV-Vis absorbance measurements show that the bandgaps of these multiphases range between 2.13-2.31 eV.

Although oxynitrides obtained from low crystallized scheelite-type YTaO₄ have better visible light absorption properties, these materials do not show any significant photoactivity towards water oxidation. On the contrary, the N-doped YTaO₄, perovskite main phase, and fluorite main phase derived from crystalline fergusonite YTaO₄ exhibit interesting photoelectrochemical performances. Loading IrO_x cocatalyst improves the photocurrent of N-doped YTaO₄ by almost 20 times, enabling the performance to be comparable to other well-known oxynitrides. This work identifies N-doped YTaO₄ as a new material showing promising potentials for solar water splitting.

■ ACKNOWLEDGEMENTS

This research is supported by the Paul Scherrer Institute and the NCCR MARVEL, funded by the Swiss National Science Foundation.

■ ASSOCIATED CONTENT

●, Supporting Information

Electronic Supporting Information (ESI) available: XRD patterns of ammonolysis products when using NaCl; TG results; DFT calculation of band gaps. See DOI: 10.1039/x0xx00000x

■ AUTHOR INFORMATION

Corresponding Author

Contact information for the author(s) to whom correspondence should be addressed.

thomas.lippert@psi.ch; daniele.pergolesi @psi.ch

Present Addresses

† present address for F. Haydous is Division of Applied Physical Chemistry, Department of Chemistry, KTH – Royal Institute of Technology, 11428 Stockholm, Sweden.

■ REFERENCES

1. Pichler, M.; Si, W.; Haydous, F.; Téllez, H.; Druce, J.; Fabbri, E.; Kazzi, M. E.; Döbeli, M.; Ninova, S.; Aschauer, U., et al. LaTiO_xN_y Thin Film Model Systems for Photocatalytic Water Splitting: Physicochemical Evolution of the Solid–Liquid Interface and the Role of the Crystallographic Orientation. *Adv. Funct. Mater.* **2017**, *27*, 1605690.
2. Osterloh, F. E. Inorganic Materials as Catalysts for Photochemical Splitting of Water. *Chem. Mater.* **2008**, *20*, 35-54.
3. Higashi, M.; Domen, K.; Abe, R. Fabrication of Efficient TaON and Ta₃N₅ Photoanodes for Water Splitting under Visible Light Irradiation. *Energy Environ. Sci.* **2011**, *4*, 4138-4147.
4. Haydous, F.; Si, W.; Guzenko, V. A.; Waag, F.; Pomjakushina, E.; El Kazzi, M.; Sévery, L.; Wokaun, A.; Pergolesi, D.; Lippert, T. Improved Photoelectrochemical Water Splitting of CaNbO₂N Photoanodes by CoPi Photodeposition and Surface Passivation. *J. Phys. Chem. C* **2019**, *123*, 1059-1068.
5. Maeda, K.; Domen, K. Photocatalytic Water Splitting: Recent Progress and Future Challenges. *J. Phys. Chem. Lett.* **2010**, *1*, 2655-2661.
6. Si, W.; Pergolesi, D.; Haydous, F.; Fluri, A.; Wokaun, A.; Lippert, T. Investigating the Behavior of Various Cocatalysts on LaTaON₂ Photoanode for Visible Light Water Splitting. *Phys. Chem. Chem. Phys.* **2017**, *19*, 656-662.
7. Pichler, M.; Szlachetko, J.; Castelli, I. E.; Marzari, N.; Döbeli, M.; Wokaun, A.; Pergolesi, D.; Lippert, T. Determination of Conduction and Valence Band Electronic Structure of LaTiO_xN_y Thin Film. *ChemSusChem* **2017**, *10*, 2099-2106.
8. Haydous, F.; Döbeli, M.; Si, W.; Waag, F.; Li, F.; Pomjakushina, E.; Wokaun, A.; Gökce, B.; Pergolesi, D.; Lippert, T. Oxynitride Thin Films versus Particle-Based Photoanodes: A Comparative Study for Photoelectrochemical Solar Water Splitting. *ACS Appl. Energy Mater.* **2019**, *2*, 754-763.
9. Castelli, I. E.; Landis, D. D.; Thygesen, K. S.; Dahl, S.; Chorkendorff, I.; Jaramillo, T. F.; Jacobsen, K. W. New Cubic Perovskites for One- and Two-Photon Water Splitting Using the Computational Materials Repository. *Energy Environ. Sci.* **2012**, *5*, 9034-9043.
10. Castelli, I. E.; Olsen, T.; Datta, S.; Landis, D. D.; Dahl, S.; Thygesen, K. S.; Jacobsen, K. W. Computational Screening of Perovskite Metal Oxides for Optimal Solar Light Capture. *Energy Environ. Sci.* **2012**, *5*, 5814-5819.
11. Li, W.; Ionescu, E.; Riedel, R.; Gurlo, A. Can We Predict the Formability of Perovskite Oxynitrides from Tolerance and Octahedral Factors? *J. Mater. Chem. A* **2013**, *1*, 12239-12245.

12. Maillard, P.; Tessier, F.; Orhan, E.; Chevire, F.; Marchand, R. Thermal Ammonolysis Study of the Rare-Earth Tantalates RTaO₄. *Chem. Mater.* **2005**, *17*, 152-156.
13. Schilling, H.; Wolff, H.; Dronskowski, R.; Lerch, M. Fluorite-Type Solid Solutions in the System Y-Ta-O-N: A Nitrogen-Rich Analogue to Yttria-Stabilized Zirconia (YSZ). In *Zeitschrift für Naturforschung B*, 2006; Vol. 61, p 660.
14. Wolff, H.; Schilling, H.; Lerch, M.; Dronskowski, R. A Density-Functional and Molecular-Dynamics Study on the Physical Properties of Yttrium-Doped Tantalum Oxynitride. *J. Solid State Chem.* **2006**, *179*, 2265-2270.
15. Maillard, P.; Merdrignac-Conanec, O.; Tessier, F. Characterization of Fluorite-Type Oxynitride Phases in the R₂TaON System (R=Rare-Earth Element). *Mater. Res. Bull.* **2008**, *43*, 30-37.
16. Muraoka, K.; Kumagai, H.; Eguchi, M.; Ishitani, O.; Maeda, K. A Z-Scheme Photocatalyst Constructed with an Yttrium-Tantalum Oxynitride and a Binuclear Ru(ii) Complex for Visible-Light CO₂ Reduction. *Chem. Commun.* **2016**, *52*, 7886-7889.
17. Tessier, F.; Marchand, R. Ternary and Higher Order Rare-Earth Nitride Materials: Synthesis and Characterization of Ionic-Covalent Oxynitride Powders. *J. Solid State Chem.* **2003**, *171*, 143-151.
18. Hisatomi, T.; Kubota, J.; Domen, K. Recent Advances in Semiconductors for Photocatalytic and Photoelectrochemical Water Splitting. *Chem. Soc. Rev.* **2014**, *43*, 7520-7535.
19. Zhao, Y.; Hernandez-Pagan, E. A.; Vargas-Barbosa, N. M.; Dysart, J. L.; Mallouk, T. E. A High Yield Synthesis of Ligand-Free Iridium Oxide Nanoparticles with High Electrocatalytic Activity. *J. Phys. Chem. Lett.* **2011**, *2*, 402-406.
20. Brixner, L. On the Structural and Luminescent Properties of the M' LnTaO₄ Rare Earth Tantalates. *J. Electrochem. Soc.* **1983**, *130*, 2435-2443.
21. Wolten, G. M. The Structure of the M' -Phase of YTaO₄, a Third Fergusonite Polymorph. *Acta Crystallogr.* **1967**, *23*, 939-944.
22. Brixner, L. H. New X-Ray Phosphors. *Mater. Chem. Phys.* **1987**, *16*, 253-281.
23. Hwang, M. H.; Kim, Y. J. Luminescent Properties of Eu³⁺-Doped YTaO₄ Powders. *Ceram. Int.* **2008**, *34*, 1117-1120.
24. Takata, T.; Lu, D.; Domen, K. Synthesis of Structurally Defined Ta₃N₅ Particles by Flux-Assisted Nitridation. *Cryst. Growth Des.* **2011**, *11*, 33-38.
25. Fuertes, A. Chemistry and Applications of Oxynitride Perovskites. *J. Mater. Chem.* **2012**, *22*, 3293-3299.
26. Moriya, Y.; Takata, T.; Domen, K. Recent Progress in the Development of (Oxy)nitride Photocatalysts for Water Splitting under Visible-Light Irradiation. *Coord. Chem. Rev.* **2013**, *257*, 1957-1969.
27. Landsmann, S.; Maegli, A. E.; Trottmann, M.; Battaglia, C.; Weidenkaff, A.; Pokrant, S. Design Guidelines for High-Performance Particle-Based Photoanodes for Water Splitting: Lanthanum Titanium Oxynitride as a Model. *ChemSusChem* **2015**, *8*, 3451-3458.
28. Park, N.-Y.; Kim, Y.-I. Morphology and Band Gap Variations of Oxynitride LaTaON₂ Depending on the Ammonolysis Temperature and Precursor. *J. Mater. Sci.* **2012**, *47*, 5333-5340.
29. Zhang, L.; Song, Y.; Feng, J.; Fang, T.; Zhong, Y.; Li, Z.; Zou, Z. Photoelectrochemical Water Oxidation of LaTaON₂ under Visible-Light Irradiation. *Int. J. Hydrogen Energy* **2014**, *39*, 7697-7704.
30. Yang, J.; Wang, D.; Han, H.; Li, C. Roles of Cocatalysts in Photocatalysis and Photoelectrocatalysis. *Acc. Chem. Res.* **2012**, *46*, 1900-1909.

31. Higashi, M.; Domen, K.; Abe, R. Fabrication of an Efficient BaTaO₂N Photoanode Harvesting a Wide Range of Visible Light for Water Splitting. *J. Am. Chem. Soc.* **2013**, *135*, 10238-10241.
32. Ueda, K.; Kato, H.; Kobayashi, M.; Hara, M.; Kakihana, M. Control of Valence Band Potential and Photocatalytic Properties of Na_xLa_{1-x}TaO_{1+2x}N_{2-2x} Oxynitride Solid Solutions. *J. Mater. Chem. A* **2013**, *1*, 3667-3674.

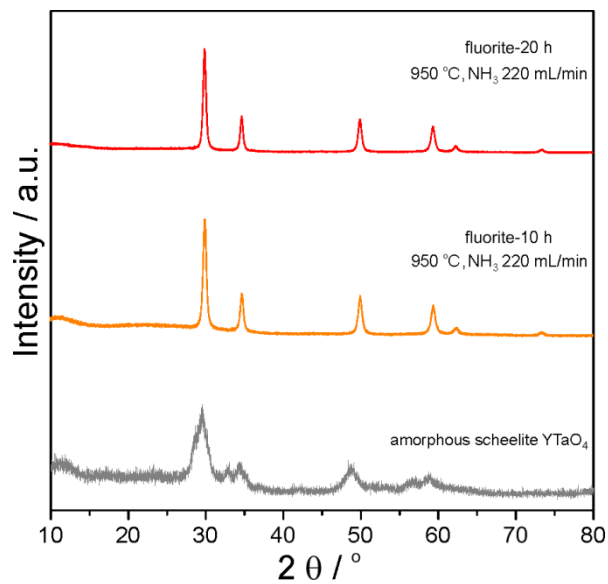


Figure 1. XRD patterns of low crystallized scheelite-type YTaO_4 and the oxynitride products under various ammonolysis conditions.

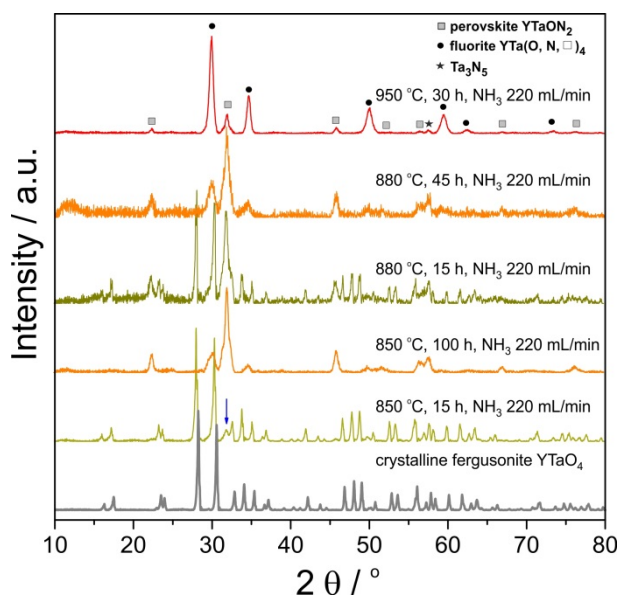


Figure 2. XRD patterns of crystalline fergusonite YTaO_4 and the oxynitride products under various ammonolysis conditions.

Table 1. Preparation conditions for yttrium tantalum oxides and oxynitrides

XRD phase	denotation	color	starting material	heating treatment
Low crystallized scheelite-type YTaO_4	LO	White	$\text{Y}(\text{NO}_3)_3 \cdot 6\text{H}_2\text{O}$, TaCl_5	750 °C, air, 5 h
Crystalline fergusonite YTaO_4	CO	White	Y_2O_3 , Ta_2O_3	1400 °C, air, 10 h
Fluorite $\text{YTa}(\text{O},\text{N},\square)_4$	FN1	Yellowish orange	LO	950 °C, NH_3 220 mL min ⁻¹ , 10 h
Fluorite $\text{YTa}(\text{O},\text{N},\square)_4$	FN2	Reddish orange	LO	950 °C, NH_3 220 mL min ⁻¹ , 20 h
N-doped YTaO_4	NO	Yellow	CO	850 °C, NH_3 220 mL min ⁻¹ , 15 h
Perovskite (main phase), fluorite and a small trace of Ta_3N_5	PM1	Yellowish orange	CO	850 °C, NH_3 220 mL min ⁻¹ , 100 h
Perovskite (main phase), fluorite and a small trace of Ta_3N_5	PM2	Yellowish orange	CO	880 °C, NH_3 220 mL min ⁻¹ , 45 h
Perovskite, fluorite (main phase) and a small trace of Ta_3N_5	FM	Reddish orange	CO	950 °C, NH_3 220 mL min ⁻¹ , 30 h

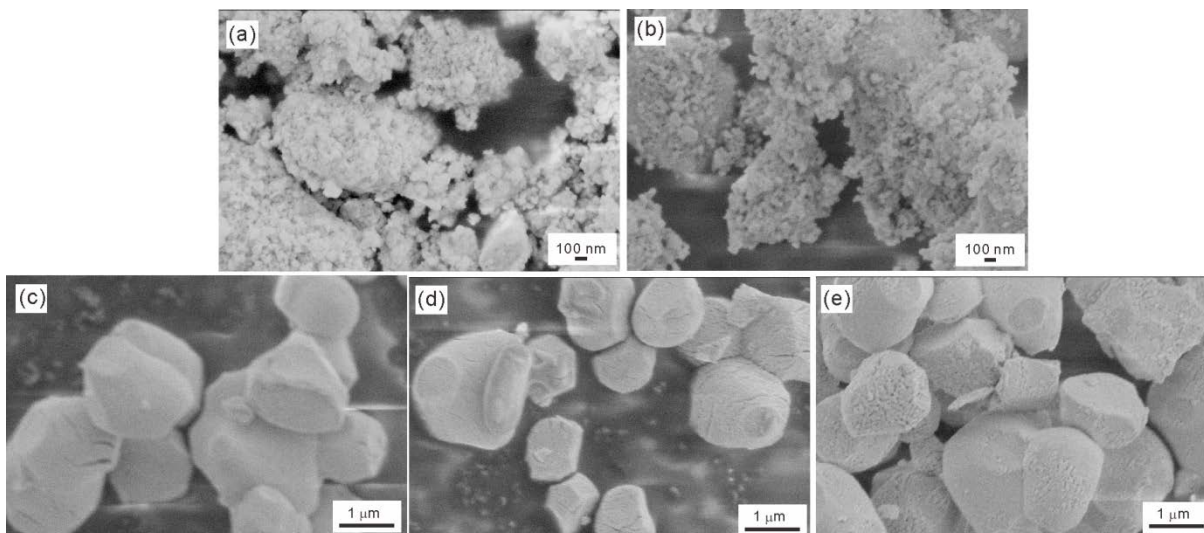


Figure 3. SEM images of Y-Ta-O-N multiphases: (a-b) obtained from precursor LO: FN1, FN2. (c-e) from precursor CO: NO, PM1, FM.

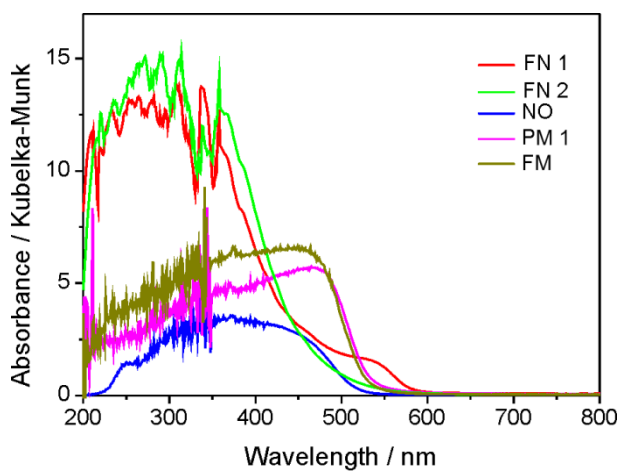


Figure 4. Kubelka-Munk absorbance of Y-Ta-O-N with different structures.

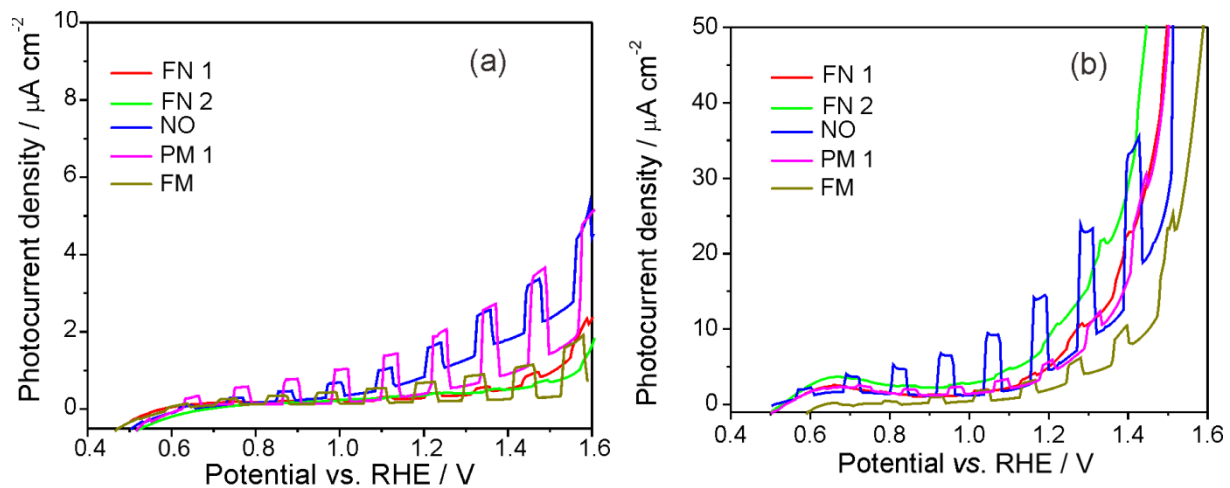


Figure 5. PEC performances in 0.5 M NaOH electrolyte (pH=13.0) under AM 1.5G illumination.

(a) Y-Ta-O-N powders with different structures, and (b) after loading of IrO_x cocatalysts.